Presented at the "Second Intern. Symp. on Hadron Structure and Multiparticle Production", Kazimierz, May 1979.

ISTITUTO NAZIONALE DI FISICA NUCLEARE
Laboratori Nazionali di Frascati

LNF-79/53(P)
28 Agosto 1979

G. Bellettini: PRODUCTION OF LEPTON PAIRS AT THE ISR.

Servizio Documentazione
dei Laboratori Nazionali di Frascati
Cas. Postale 13 - Frascati (Roma)

INFN - Laboratori Nazionali di Frascati
Servizio Documentazione

LNF-79/53(P)
28 Agosto 1979

G. Bellettini(+): PRODUCTION OF LEPTON PAIRS AT THE ISR.

(Review talk at the Second International Symposium on Hadron Structure and Multiparticle Production, Kazimierz, 20-26 May 1979).

Inclusive studies of lepton pair production in proton-proton collisions have lead to hystorical triumphs, the discovery of the J and Y particles at BNL and FNAL. These studies are also intensively pursued at the CERN ISR where $\sqrt{s}$ can reach 62 GeV and l^+l^- systems with $M_{l^+l^-} \gtrsim$ 30 GeV can be readily produced in inelastic collisions. The energy should be enough to produce the lowest $t\bar{t}$ state of the hypotetical top quark. Although this state has untill now escaped detection, the ISR date are providing important information on a) the energy dependence of the non-resonant lepton-pair cross-section (Drell-Yan scaling), b) the energy dependence of the Y excitation cross-section, and c) the correlation between massive lepton pairs and the associated hadrons.

(+) INFN, Sezione di Pisa, Istituto di Fisica dell'Università di Pisa, and INFN, Laboratori Nazionali di Frascati.

DRELL-YAN SCALING.

The assumption is made[1] that the lepton pairs are produced in the fusion of a quark of one proton with a (sea) antiquark of the other proton. The data are indeed consistent with this mechanism being dominant. The reaction $p + p \longrightarrow l^+l^- +$ anything is schematized as is schematized as

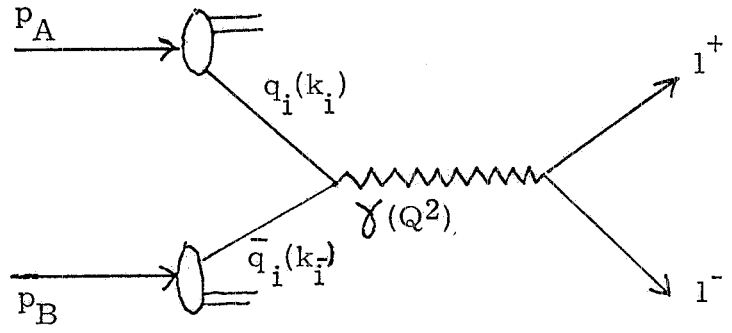

where two quarks of tipe i (and the same colour) with momenta k_i, $k_{\bar{i}}$ annihilate into a virtual γ of invariant squared four-momentum Q^2. Introducing the fractions x_i, $x_{\bar{i}}$ of the original proton momenta p_A, p_B carried by the two quarks

$$k_i = x_i\, p_A, \quad k_{\bar{i}} = x_{\bar{i}}\, p_B$$

one can express the squared mass of the produced $l^+ l^-$ system as (neglecting masses and transverse momenta relative to longitudinal momenta)

$$m^2 = Q^2 = (k_i + \bar{k}_i)^2 = (x_i\, p_A + x_{\bar{i}}\, p_B)^2 = x_i\, x_{\bar{i}}\, s$$

where $s = (E_A + E_B)^2$ is the total energy squared of the proton-proton reaction.

The fractional energy carried away by the lepton pair is

$$\sqrt{\tau} = \frac{m}{\sqrt{s}} = x_i\, x_{\bar{i}}$$

and the longitudinal momentum of the pair relative to the beam momen

tum is:

$$X_F = \frac{2\, p_{\parallel}\,,\, l^+l^-}{\sqrt{s}} = x_i - x_{\bar{i}} \ .$$

The Drell-Yan cross-section is obtained as a convolution of the quark annihilation cross-section $\sigma(q_i \bar{q} \longrightarrow l^+ l^- p$ over the quark momentum distribution, summed over all quark types, i. e.(for a collision between two identical protons, and N_C quark colours)

$$\frac{d}{dm^2}(pp \rightarrow l^+l^- + \text{anything}) =$$

$$= \frac{2}{N_C}\sum_i \iint dx\, dy\, f_i(x) f_{\bar{i}}(y) \sigma(q_i \bar{q}_i \rightarrow l^+l^-) \delta(m^2 - xys).$$

The cross-section $(q_i \bar{q}_i \rightarrow l^+l^-)$ is the same as in $e^+e^- \rightarrow \mu^+\mu^-$, except for a weight factor e_i^2 ($e_i^2 = 1/9$ or $4/9$ depending on the quark type):

$$\sigma(q_i \bar{q}_i \rightarrow l^+l^-) = e_i^2 \frac{4\pi\alpha^2}{3m^2}$$

Thus

$$\frac{d\sigma}{dm^2} = \frac{2}{N_C} \frac{4\pi\alpha^2}{3m^4} \sum_i e_i^2 \iint dx\, dy\, f_i(x) f_{\bar{i}}(y)\, \delta\left(1 - \frac{xy}{\tau}\right).$$

Since integration gives a function of τ, this formula predicts scaling:

$$m^4 \frac{d\sigma}{dm^2} \left(\text{or } \frac{m^3}{2} \frac{d\sigma}{dm}\right) = F(\tau), \text{ independent of s.}$$

Using $X_F = x - y$ one also derives

$$\frac{d\sigma}{dm^2 dX_F} = \frac{2}{N_C} \frac{4\pi\alpha^2}{3m^4} \frac{\tau}{\sqrt{X_F^2 + 4\tau}} \sum_i e_i^2 f_i\left(\frac{\sqrt{X_F^2+4\tau}+X_F}{2}\right) f_{\bar{i}}\left(\frac{\sqrt{X_F^2+4\tau}-X_F}{2}\right),$$

$$m^4 \frac{d\sigma}{dm^2 dX_F} = G(\tau, X_F), \text{ independent of s.}$$

Notice that $d\sigma/dm^2 dX_F$ factorizes in the quark (or valence) and anti-quark (sea) distributions in the proton. A study of scaling of these cross-sections up to ISR energies will allow to compaire the quark distribution functions -primarily the sea one- at very large Q^2 with those derived from deep inelastic lepton scattering. This study shows qualitative consistency at FNAL energies[2].

Often in practice the cross-section $d\sigma/dmdy$ (y=rapidity of the pair) is more readily derived from the data rather than $d\sigma/dm$. For a quantitative (although not very precise) comparison between these functions one can proceed as follows[3]. Notice that

$$\left.\frac{d\sigma}{dm\ dy}\right|_{y=0} = 2\tau \left.\frac{d\sigma}{dm\, dX_F}\right| X_F=0 \qquad (\text{for } m_{l^+l^-} \gg p_{\perp,l^+l^-}).$$

A study of the X_F- dependence of the cross section in the CERN-HARWARD-Frascati - MIT - Naples - Pisa Collaboration at the ISR shows that

$$\frac{d\sigma}{dm\ dX_F} \qquad \left.\frac{d\sigma}{dm\, dX_F}\right| X_F=0 \quad (1 - X_F)^{2.8}.$$

This formula can be integrated over X_F to give $d\sigma/dm$. Thus one gets

$$\left.\frac{d\sigma}{dm\, dy}\right| y=0 \approx 3.8\tau \frac{d\sigma}{dm} \quad .$$

THE ISR LEPTON PAIR EXPERIMENTS.[4]

Table I summarizes a few parameters of the three ISR experiments that are producing more relevant information on lepton pairs: R 108 (CERN-Columbia-Oxford-Rochfeller Collaboration), R 806 (Athens BNL-CERN-Syracuse Collaboration), R 209 (CERN-Hardward - Frascati- MIT--Naples-Pisa Collaboration).

TABLE I - Parameters of ISR lepton-pair experiments.

Experiment	R 108	R 806	R 209
$\Delta\Omega$	4 sr	4 sr	8 sr
technique	solenoid, cylindrical chambers, Pb-glass (electron pairs)	transition radiation, liquid Argon (electron pairs)	iron toroids, plane chambers, vertex detector (μ-pairs)
$\int L\,dt$ (data analysed as of May 1978)	8×10^{37} cm^{-2}	4×10^{37} cm^{-2}	9×10^{37} cm^{-2}

Fig. 1 gives a sketch of the R 108 detector. Cylindrical drift chambers in the longitudinal field of a superconducting solenoid measure the momenta of charged particles produced at large angles. Electrons are identified in two lead-glass walls.

Fig. 2 shows the mass spectrum of 191 opposite sign electron pairs (lower hystogram). On comparing with the e^-e^- mass spectrum of background electron pairs (upper hystogram), this data is found to be free from background for $m_{e^+e^-} \gtrsim 9$ GeV. After background subtraction and Montecarlo computation of the trigger + analysis acceptance one derives the cross-section $\frac{d\sigma}{dm\,dy}\Big|_{y=0}$ as shown in Fig. 3. The scaling function which fits the Fermilab data is found to be about 20% above the data, which is probably to be considered well compatible with scaling when uncertainties in the absolute normalization of the data are taken into account.

From the 46 events observed in the Y region one estimates, after allowing for a smooth non-resonant background.

$$\frac{\text{ipsilon signal}}{\text{continuum (9 m 10 GeV)}} = 2.8 \pm 1.2 \text{ (at } y=0)$$

and also

$$\frac{d\sigma_Y}{dy}\Big|_{y=0} B_{ee} = (9 \pm 3)\ 10^{-36}\ \text{cm}^2 \text{ at } \sqrt{s} = 62 \text{ GeV}$$

$$\frac{d\sigma_Y}{dy}\Big|_{y=0} B_{ee} = (6 \pm 3)\ 10^{-36}\ \text{cm}^2 \text{ at } \sqrt{s} = 44 \text{ GeV}.$$

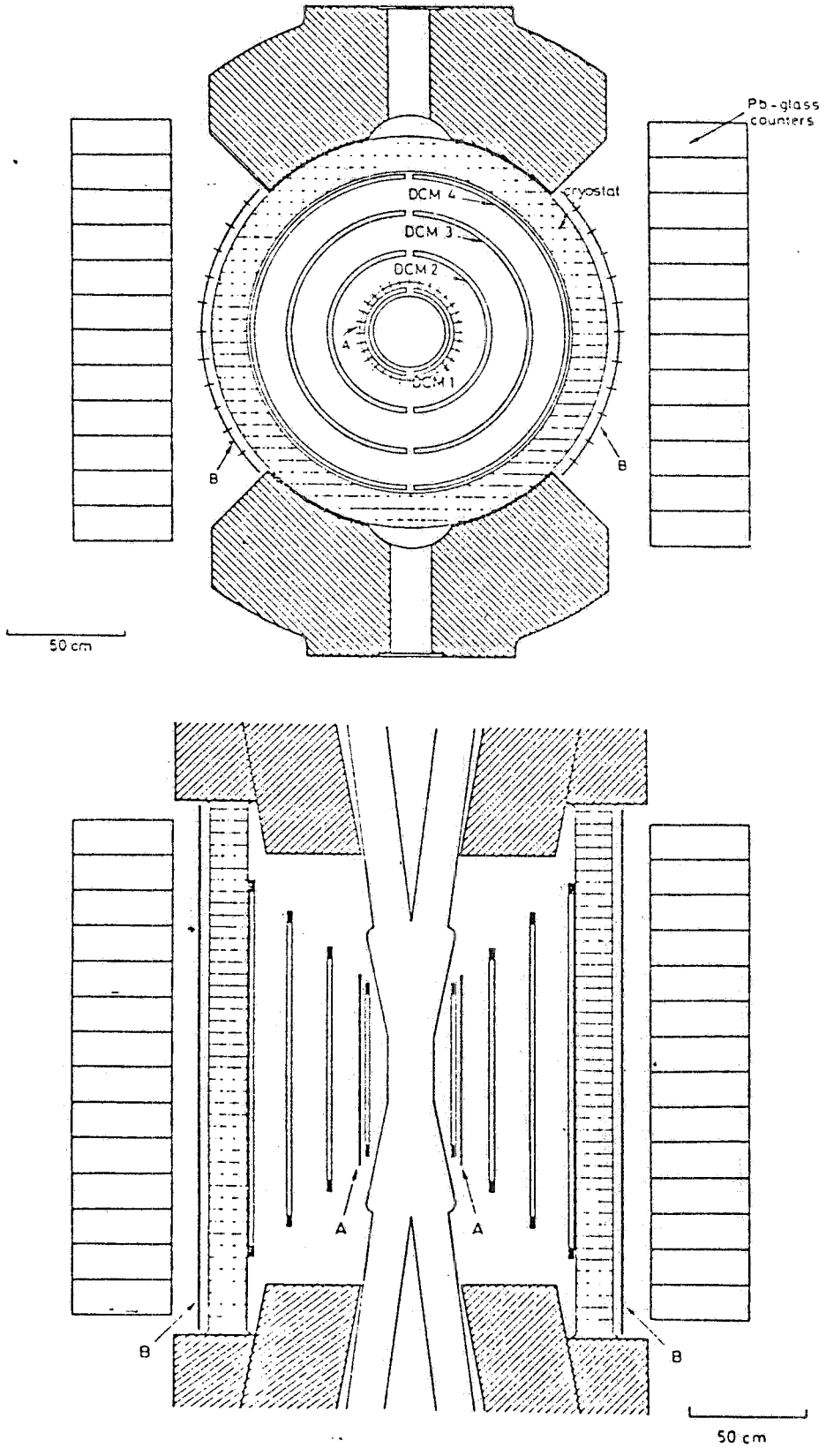

FIG. 1 - Experiment R108. CERN-Columbia-Oxford--Rockefeller Collaboration.

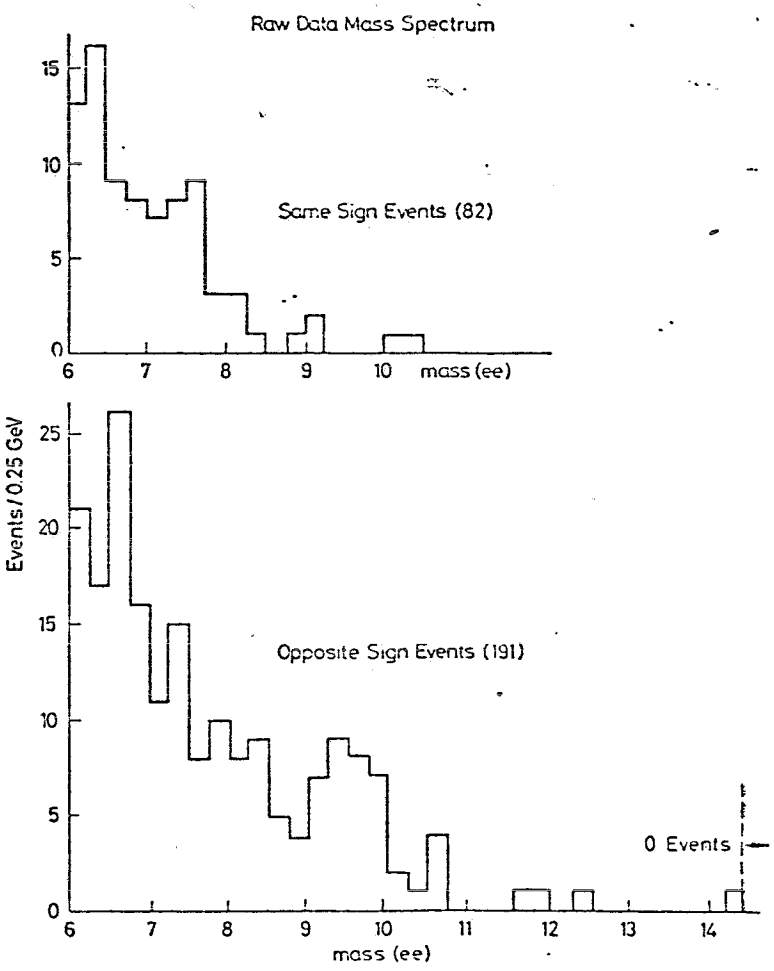

FIG. 2 - Mass spectrum of e^+e^- (lower hystogram) and e^-e^- (upper hystogram) pairs of experiment R108 (ref. (4)).

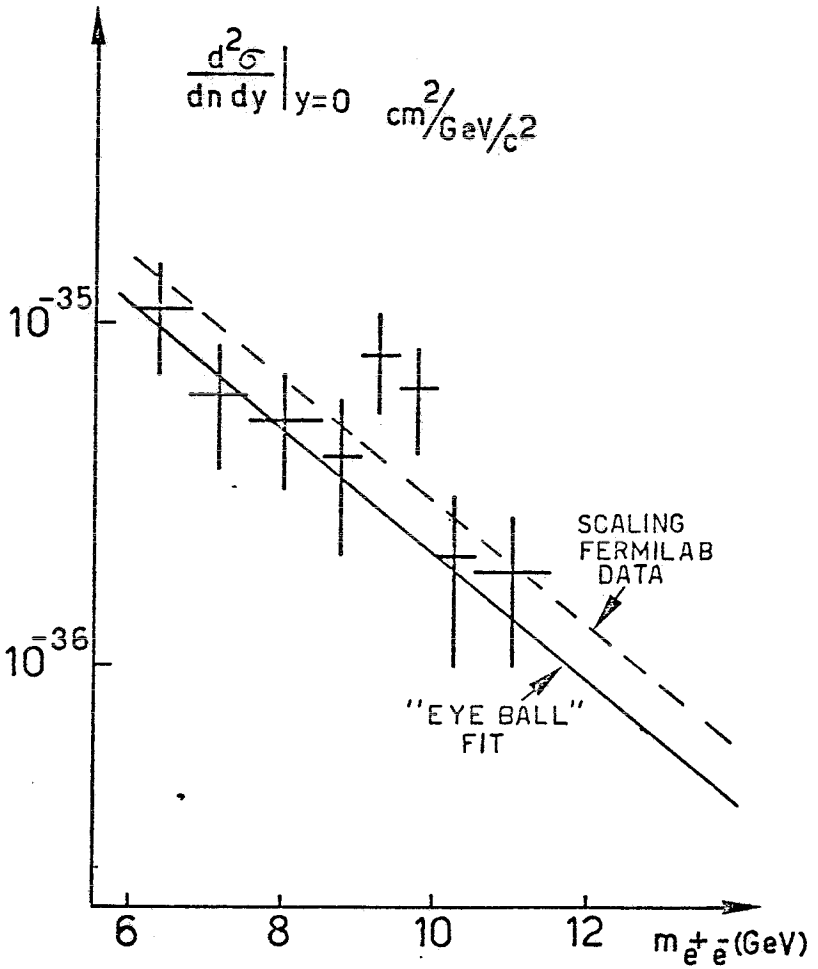

FIG. 3 - Electron pair production cross-section from experiment R108 (ref. (4)).

The average transverse momentum of the electron pairs is rather mass-independent and is around 1.5 GeV/c, as shown in Fig. 4. On the other hand, a slight decrease of the associated charge multiplicity (observed within the acceptance) is found at the Y, as seen in Fig. 5. It will be shown later, when discussing the correlation data of R 209, that this trend continues at larger masses and can be interpreted in a natural and simple way.

Fig. 6 shows a sketch of the R 806 detector. Four identical electron telescopes are set at different azimuths. Electrons are identified after a sofisticated analysis of their pulse-height in proportional wire chambers backing sandwitches of lithium transition radiators, and in the liquid argon colorimeters. At high energy the acceptance for a single electron entering a telescope is, after the trigger and analysis cuts, 36% and the signal is essentially free from background. At the Y, the electron pair mass resolution is $\pm$ 4%.

Fig. 7 shows the R 806 mass spectrum. The scaling cross-section $m^3 \frac{d\sigma}{dm\, dy}\Big|_{y=0}$ derived from the R 806 data outside the Y is plotted on the fitted curve[5] to the Columbia-Story Brook data in Fig. 8. Although the data are much poorer than the FNAL data, one remarks that they satisfy scaling very well.

For the 52 ee events observed in the Y region in the combined $\sqrt{s}$ = =53 and $\sqrt{s}$ = 62 GeV data one estimates

$$\frac{\text{ipsilon signal}}{\text{continuum } (9 < m_{e\,e} < 10 \text{ GeV})} = 4.5 \pm 1.5 \text{ (at } y=0)$$

and

$$\frac{d\sigma_Y}{dy}\Big|_{y=0} B_{ee} = (14 \pm 8)\, 10^{-36}\ \text{cm}^2 \text{ at } \sqrt{s}\ 53 \text{ GeV}$$

$$\frac{d\sigma_Y}{dy}\Big|_{y=0} B_{ee} = (15.2 \pm 5.5)\, 10^{-36}\ \text{cm}^2 \text{ at } \sqrt{s} = 62 \text{ GeV}.$$

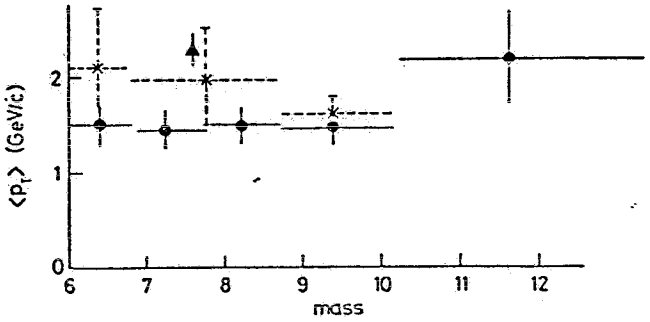

FIG. 4 - Mean transverse momentum of e^+e^- pairs, from experiment R108. ⧫ : $\pi^o\pi^o$ events; ⧫: data from experiment R806 (ref. (4)).

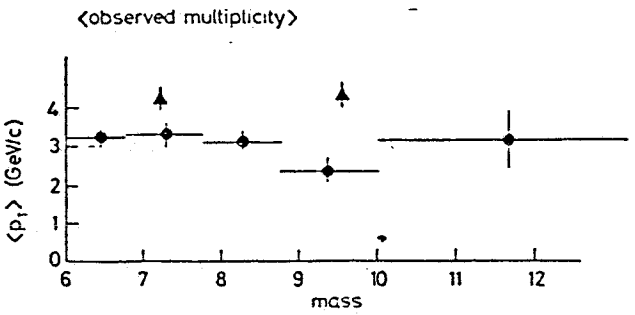

FIG. 5 - Average charge multiplicity associated to the e^+e^- pairs, observed in the (large angle) detector of R108. ⧫ : $\pi^o\pi^o$ events.

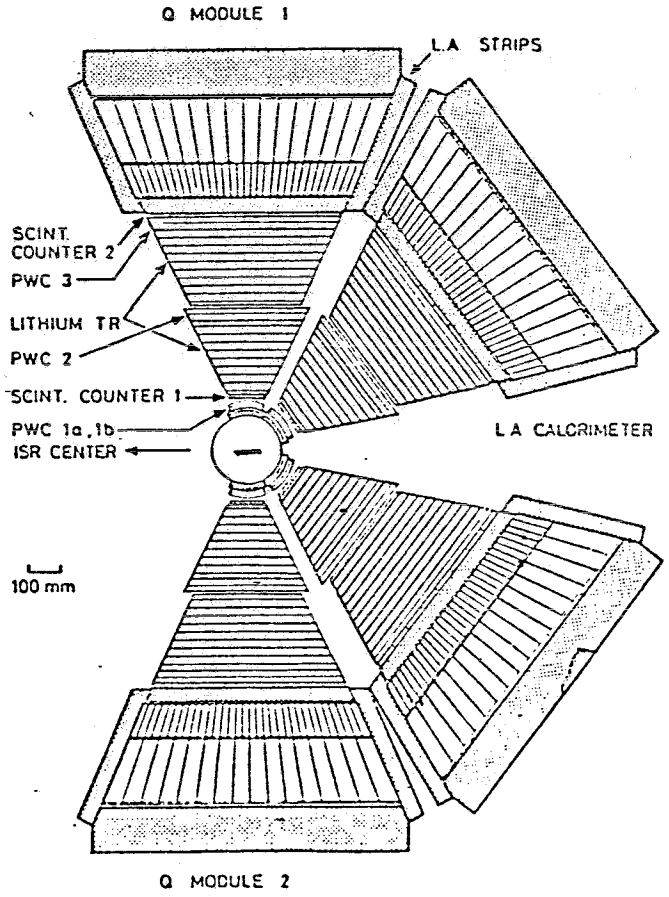

FIG. 6 - Experiment R806. Athens-BNL-CERN--Syracuse Collaboration.

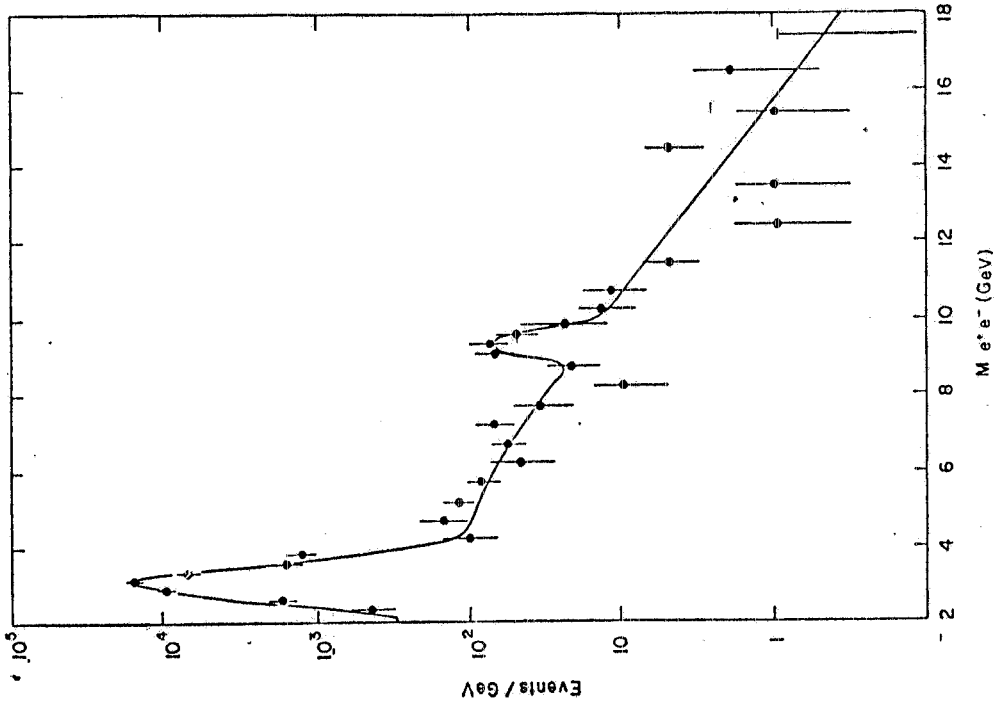

FIG. 7 - Mass spectrum of electron pairs, from experiment R806 (ref.(4)).

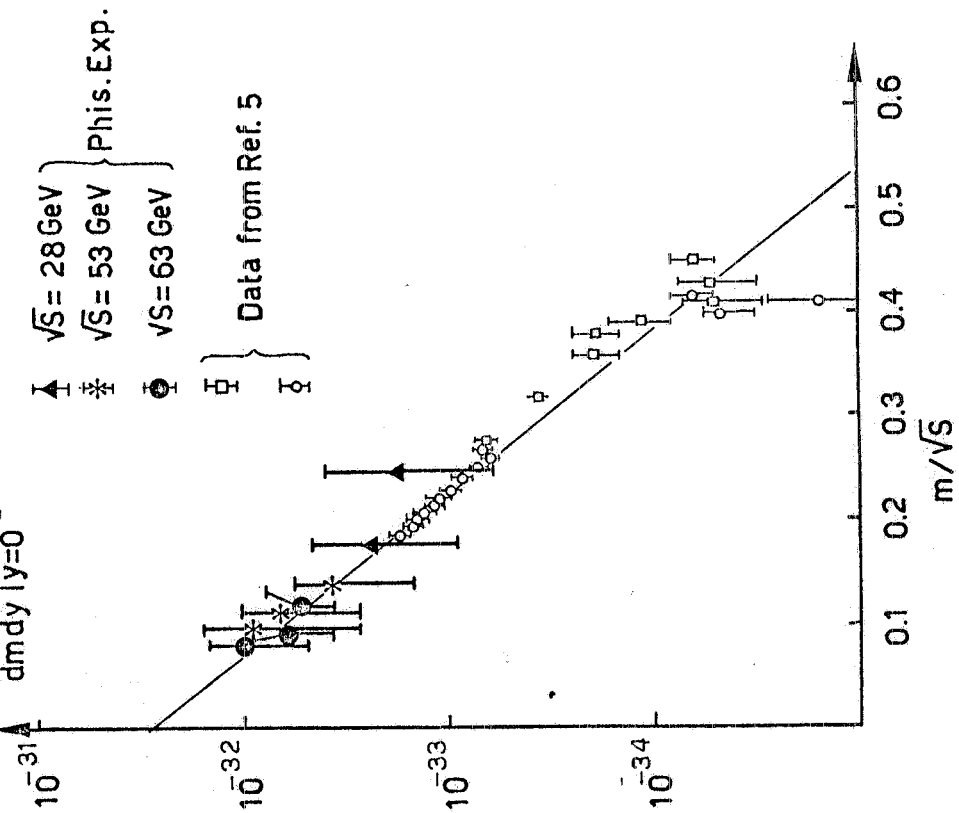

FIG. 8 - Scaling cross-section from experiment R806. ▲: FNAL data; ⊡: BNL data, See ref. (5) (ref.(4)).

The dependence of $\frac{d\sigma_Y}{dy}\Big|_{y=0} B_{ee}$ on the scaling variable τ is shown in Fig. 9, which includes FNAL data at lower energies (and larger τ's), and allows a comparison with the J/ψ excitation cross-section. One finds a steeper τ dependence for the Y:

$$\frac{d\sigma_Y}{dy}\Big|_{y=0} \propto e^{-18\sqrt{\tau}}$$

while

$$\frac{d\sigma_{J/\psi}}{dy}\Big|_{y=0} \propto e^{-14.5\sqrt{\tau}}$$

A sketch of the R 209 detector is shown in Fig. 10. Muons are filtered and bent in iron toroids, and their momenta is measured with the aid of large size drift chambers. A break-up of the central detector, which comparises over 140 small size modular drift chambers assembled in lateral and forward telescopes, is shown in Fig. 11. In addition to the μ-pairs, this box detects over 90% of the associated charged hadrons. Hadrons are also detected in forward drift chambers.

The acceptance of the R 209 detectos is very small at the J/ψ, grows smoothly at larger masses and reaches a constant value of $\approx$ 15% for m $\gtrsim$ 10 GeV. An uncertainty of about $\pm$ 25% has to be attributed to this computed efficiency because of uncertainties in the $p_\perp$ and X_F dependence of the μ-pair production cross-section and in the angular distribution of the muons.

The μ-pair mass resolution is computed to be $\sim \pm$ 10%, essentially independent of mass. Study of the shape of the J/ψ peak gives indeed $\frac{\Delta m}{m} = \pm$ 11%.

To allow a comparison of R 209 data with the CFS Fermilab data, one can derive scaling curve[3] for $\frac{d\sigma}{dm}$ from that data (which is quoted as $\frac{d\sigma}{dm\,dy}\Big|_{y=0}$ in the literature) using the relation $\frac{d\sigma}{dm} = \frac{}{3.8\tau} \frac{d\sigma}{dm\,dy}\Big|_{y=0}$.

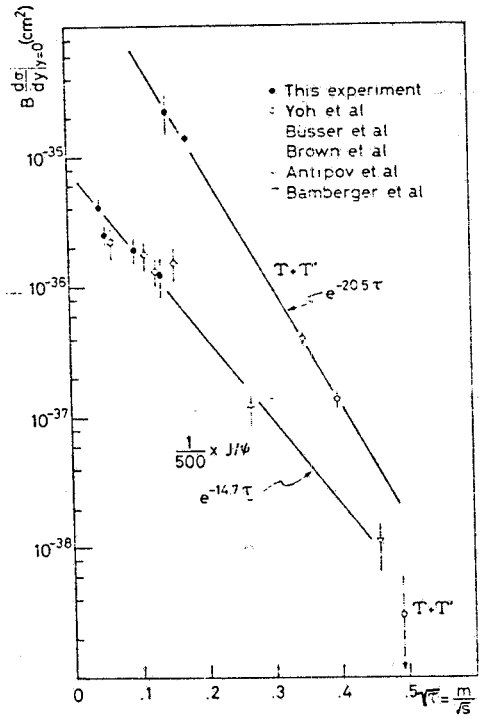

FIG. 9 - Production cross-section of the ipsilon versus $\sqrt{\tau}$, from R806 (upper plot). CFS data from Fermilab. The J/ψ cross-section is shown below for comparison (ref. (4)).

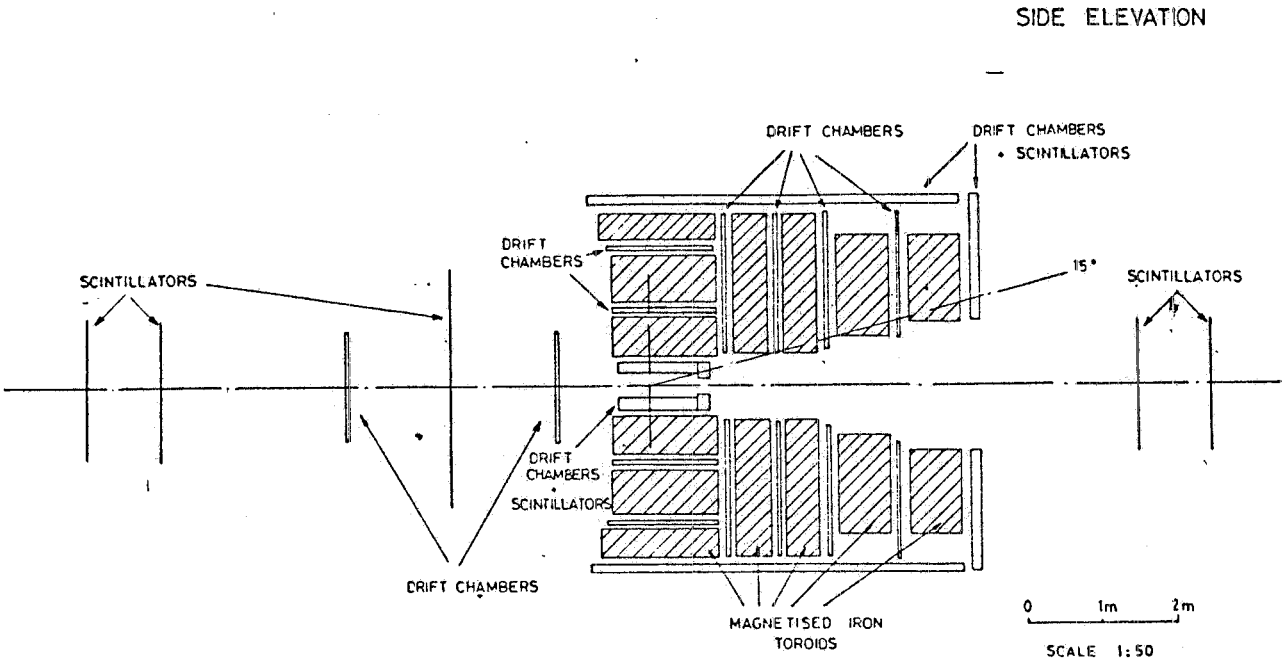

FIG. 10 - Experiment R209. CERN-Frascati-Harvard-MIT-Naples--Pisa Collaboration.

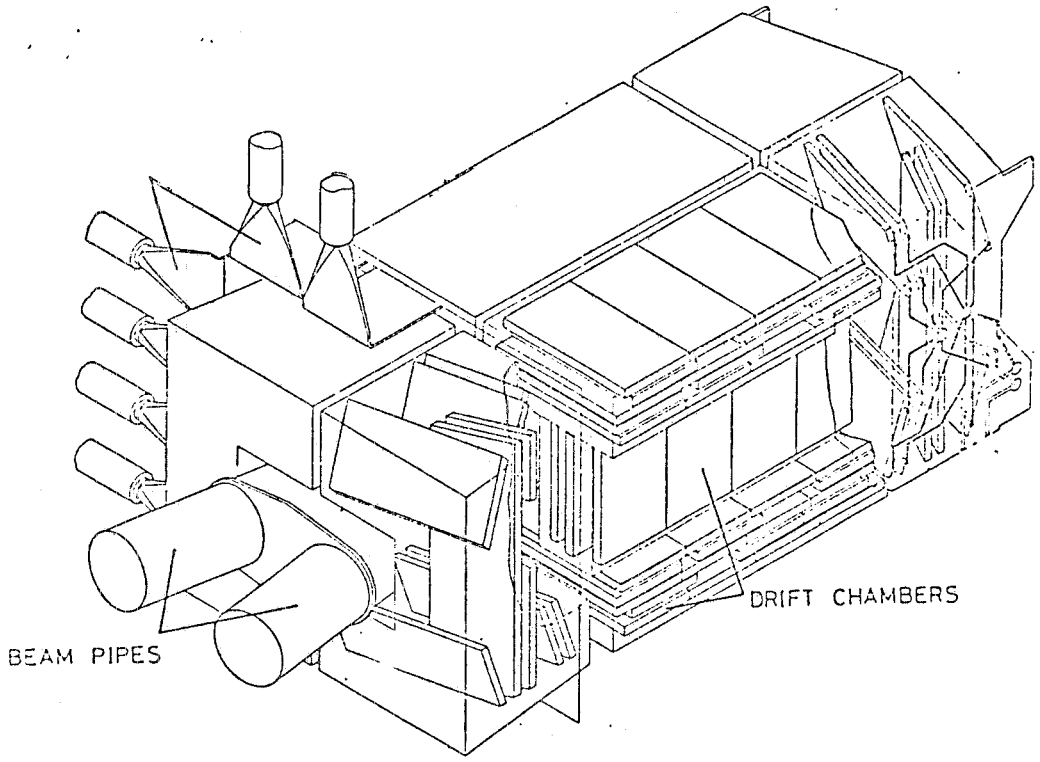

FIG. 11 - Central detector (in part) of R209.

Equally good fits are obtained for $m^3 \frac{d\sigma}{dm}$ as

$$F_1(\tau) = 13 \exp(-18.6\sqrt{\tau})\ 10^{-32}\ \text{GeV}^2\ \text{cm}^2$$

or

$$F_2(\tau) = 5,23 \left[(1-\sqrt{\tau})^{10}/\sqrt{\tau}\right]\ 10^{-33}\ \text{GeV}^2\ \text{cm}^2$$

as shown in Fig. 12. This fit is compaired with the R 209 data of the Tokyo Conference[6] ($\int L\,dt = 2.6 \cdot 10^{37}\ \text{cm}^2$) in Fig. 13, showing an excellent agreement with scaling from FNAL to ISR. Note that $d\sigma/dm$ grows by as much as 30 at m = 8 GeV and 200 at m = 12 GeV. A more direct comparison with the scaling prediction is shown in Fig. 14, which gives $\frac{d\sigma}{dm\,dX_F}\Big|_{X_F \approx 0}$.

The broken curve that fits rather well the data is derived from CFS according to the relationship $\frac{d\sigma}{dm\,dX_F}\Big|_{X_F=0} = \frac{1}{2\tau}\frac{d\sigma}{dm\,dy}\Big|_{y=0}$

One sees again that scaling is well satisfied (remember, however, the estimated $\pm$ 25% uncertainty in the efficiency of R 209).

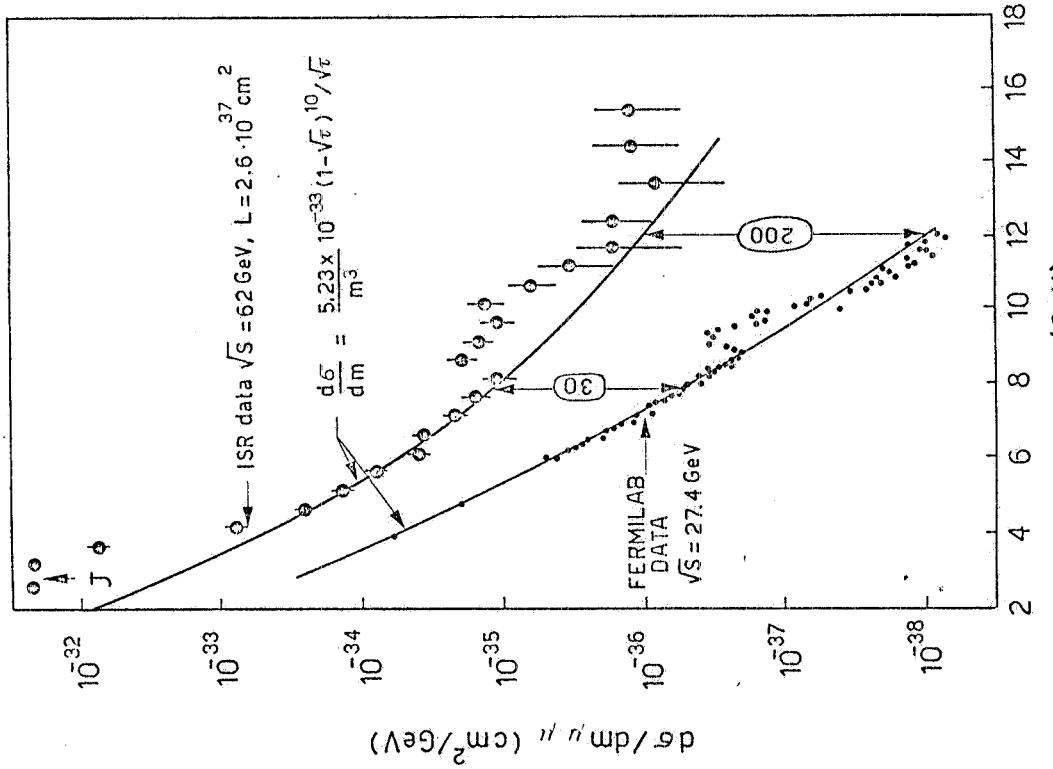

FIG. 13 - R209 mass distribution at $\sqrt{s}$ = 62 GeV, compared with the CFS Fermilab data (as at Tokyo 1978). The full curve is $1/m^3$ times the fitted scaling curve $F(\tau)$ to the converted into $d\sigma/dm$ Fermilab data.

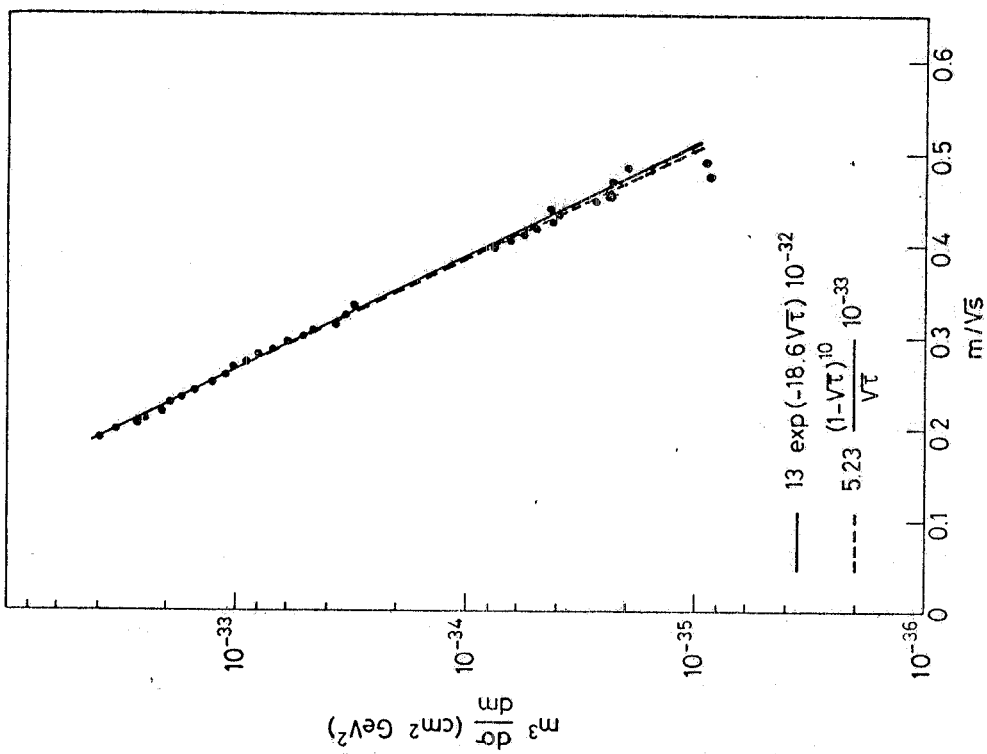

FIG. 12 - The quantity $m^3(d\sigma/dm)$ plotted versus $\sqrt{\tau}$ for the CFS data. The full line represents the fit: $F_1(\tau) = 13\exp(-18.6\sqrt{\tau})\,10^{-32}$. The dashed line represents the other fit: $F_2(\tau) = 5.23[(1-\sqrt{\tau})^{10}/\sqrt{\tau}]\,10^{-33}$ (ref. 4).

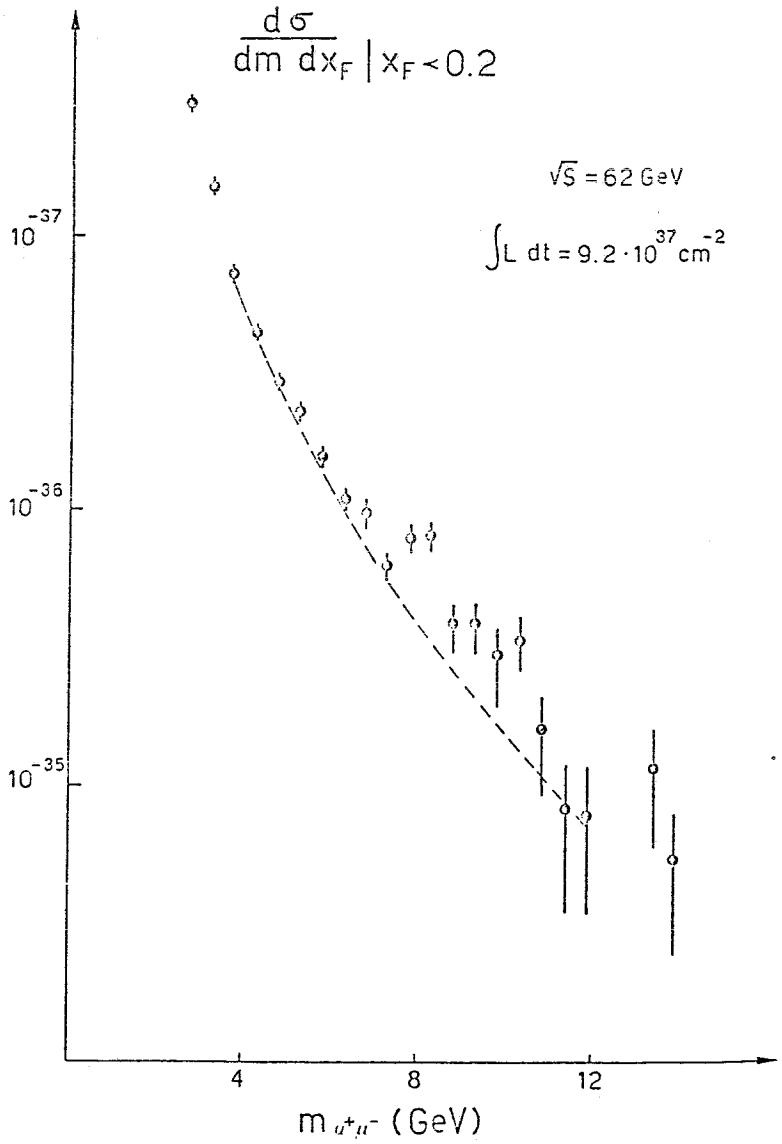

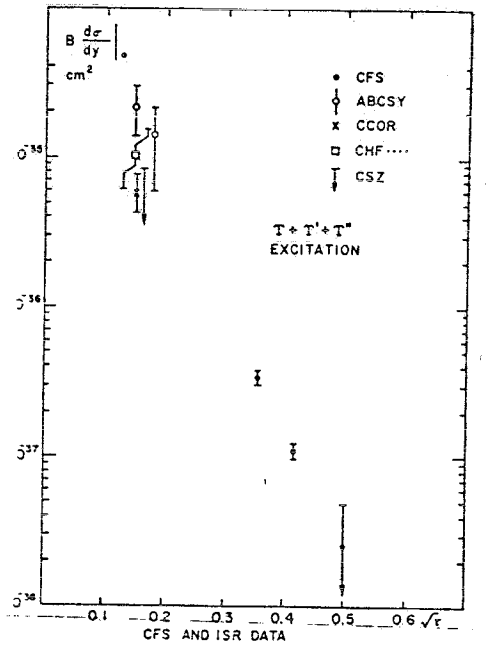

FIG. 15 - Excitation of the ipsilon from FNAL to ISR (ref. 2).

FIG. 14 - $\left.\frac{d\sigma}{dm\,dx_F}\right|_{x_F=0}$ at $\sqrt{s}$ = 62 GeV, from R209.

The broken curve is the scaled CFS cross-section.

From the excess of data in the Y region one estimates

$$\sigma_Y \cdot B = (10 \pm 3.5) 10^{-36} \text{ cm}^2 \text{ at } \sqrt{s} = 62 \text{ GeV}.$$

A compilation[2] of $\frac{d\sigma_Y}{dy}\Big|_{y=0} B_{l^+l^-}$ from Fermilab to ISR is shown in Fig. 15. Compairing this with the Drell-Yan cross-section one finds that

$$\frac{\text{ipsilon}}{\text{Continuum}} = 4 \div 6 \text{ GeV at the ISR, while one has}$$

$$\frac{\text{ipsilon}}{\text{Continuum}} = 1.26 \text{ GeV at Fermilab.}$$

The R 209 experiment observes a number of events with masses above 15 GeV, a few of which have masses as large as 25 GeV. A computer-reconstructed picture of the μ-pair of such an event is shown in Fig. 16. These events are being studied accurately in order to reject all sources of background and to derive the best measure of their kinematical parameters. However, their total rate is compatible with Drell-Yan.

It has been found at FNAL that the lepton-pair distribution in transverse momentum is too wide to be accounted for in the pure Drell-Yan mechanism. Indeed, $k_{\perp,q} \approx 400$ MeV/c is expected for each quark since they are confined in a region of size ~ 1 Fermi. Therefore one would expect a "primordial contribution $\langle p_{\perp,\mu\mu} \rangle = 2 \langle k^2_{\perp,q} \rangle$ from the fusion of two quarks. On the other hand, at the top FNAL energies $1/2 \langle p_{\perp,\mu\mu} \rangle$ is $\simeq 1$ GeV/c. This effect is tentatively understood in QCD by invoking additional dinamical effects (like gluon scattering or emission) which would produce final state μ-pairs with large $p_\perp$. In this skeme one would have

$$\langle p^2_{\perp\,\mu\mu} \rangle = \langle p^2_{\perp\,\text{primordial}} \rangle + \langle p^2_{\perp\,\text{QCD}} \rangle .$$

The chanches for QCD to explain the large $\langle p_\perp \rangle$ depend of course on the size of the effect, which is quite large already at FNAL. It is therefore particularly important to cohck the behaviour of $\langle p_{\perp,\mu\mu} \rangle$ up to ISR energies. Fig. 17 shows the preliminary $p_\perp$ distribution of R 209 at $\sqrt{s}$ =

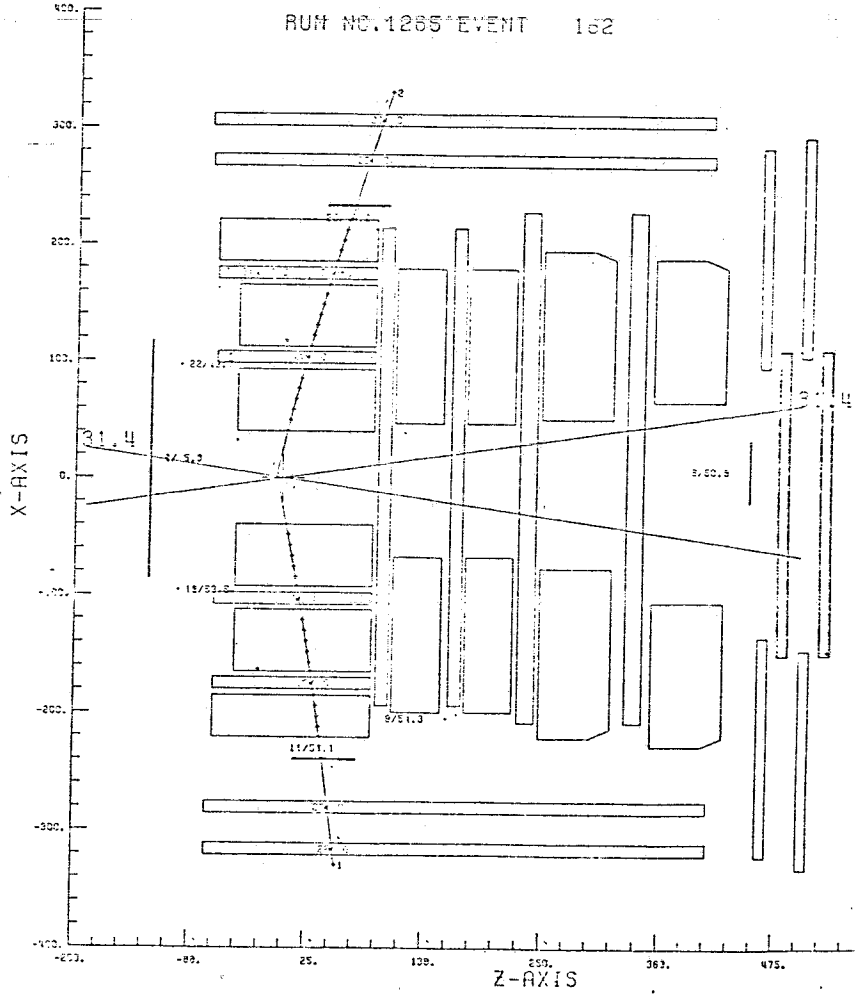

FIG. 16 - Computer-reconstructed μ-pair event of high mass in R209 (p_1 = 11 GeV/c, p_2 = 14.8 GeV/c, $m_{\mu\mu}$ = 24.9 GeV).

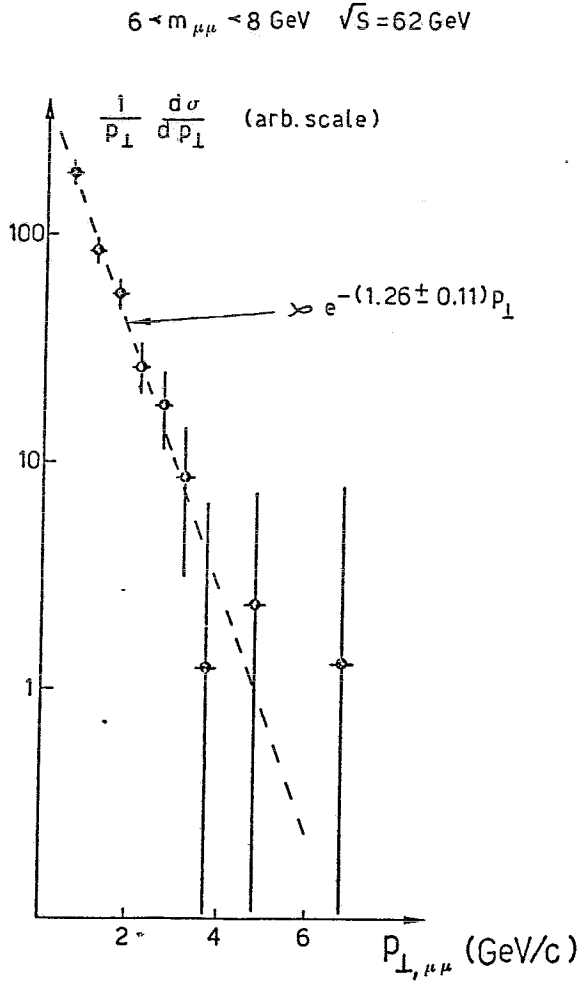

FIG. 17 - Distribution in $p_\perp$ of μ-pairs with $6 < m < 8$ GeV, from experiment R209 (preliminary).

=62 GeV which indicates that for $6 < m < 8$ GeV $< p_{\perp,\mu\mu} > \approx 1.8 \pm 0.2$ GeV/c . One sees that the increase of $< p_\perp >$ at large masses continues from FNAL to the ISR.

In QCD one expects two first order processes (in α_s) to contribute to the experimentally measured lepton pair cross-section

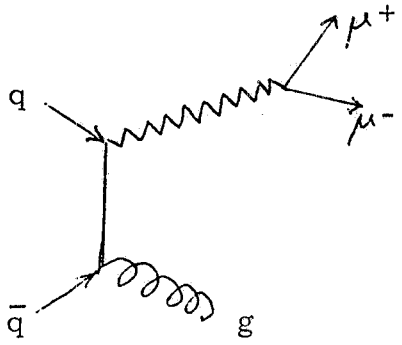

gluon bremstrahlung in $q\bar{q}$ annihilation

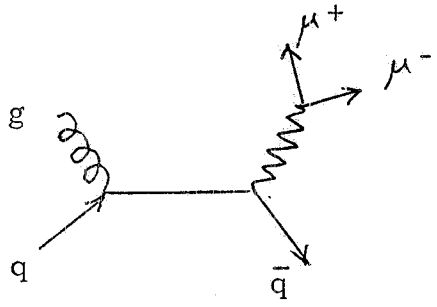

gluon-quark Compton scattering

While the scaling violation brought in by these graphs is small in view of the systematics uncertainties of the ISR experiments, they can contribute to explain the excess of large $p_\perp$ lepton pairs. The $p_\perp$ dependence of the annihilation and Compton graphs has been computed, and one finds that Compton is most effective at large $p_\perp$ and shoud dominate for $p_\perp \gtrsim 3$ GeV/c (the opposite is true in $\bar{p}p$ reactions)[7]. Since a quark recoils against the μ-pair in the Compton process, one might hope to discover features of the hadronic quark jet by studying at the ISR the hadrons produced in association to large $p_\perp$ -pairs. Fig. 18 shows a computer reconstructed view of the associated charged tracks for such an event (same event of Fig. 16). These events are being studied searching for significant sistematic trends.

Fig. 19 shows the raw mean multiplicity of charged tracks accomparing the μ-pairs observed in the R 209 central detector (which is expect to differ from the true multiplicity by no more than one unit). The decreasing

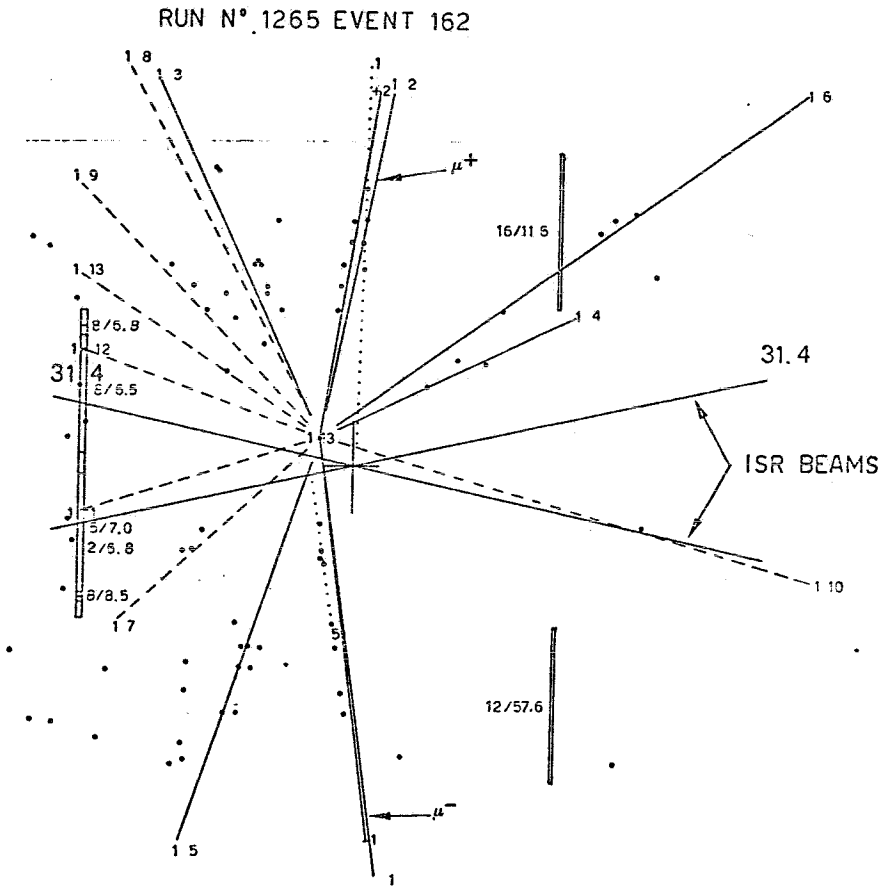

FIG. 18 - Computer reconstructed plot (top view) of the charged tracks traversing the central detector of R209 for a large mass μ-pair event (same event of Fig. 16).

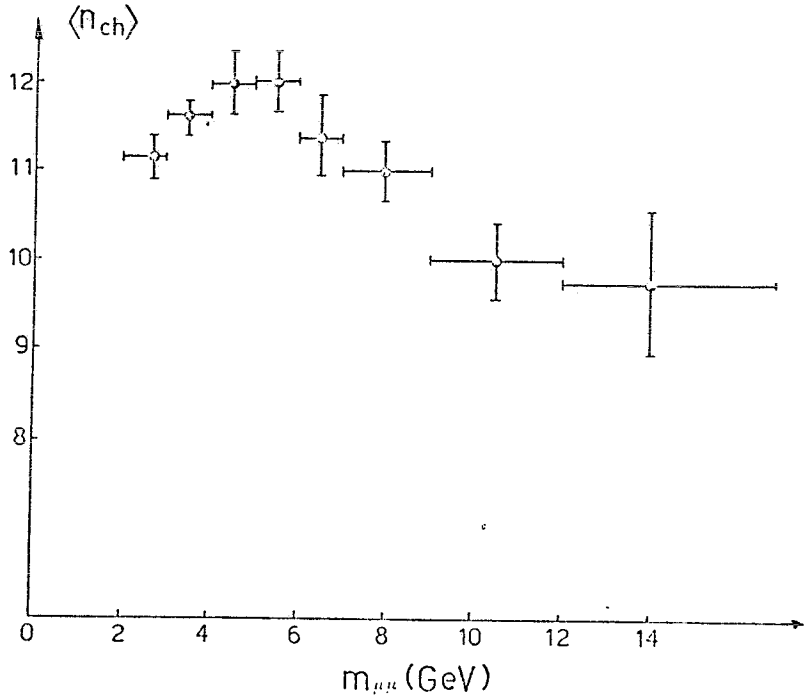

FIG. 19 - Raw mean charged multiplicity associated to heavy μ-pairs at $\sqrt{s}$ = 62 GeV, from R209 (preliminary).

$\langle n_{ch} \rangle$ for $m \gtrsim 5$ GeV can be attributed to the increasing amount of energy that the μ-pair removes from the reaction. This is seen in Fig. 20, where the same data is plotted versus the μ-pair energy.

When expressed in terms of the reduced squared energy

$$\hat{s} = (\sqrt{s} - E)^2$$

The data are consistent with the same curve which fits the inclusive ISR data[8]

$$\langle n_{ch} \rangle = a + b \ln \hat{s} + c (\ln \hat{s})^2$$

In Fig. 20 the curve at $E^*_{\mu\mu} = 0$ has been normalized to 12.2, the raw inclusive multiplicity measured in R 209 (12,8 in ref. (8)).

The dependence of the associated multiplicity on transverse momentum is shown in Fig. 21. Up to $p_\perp = 2.5$ GeV, the multiplicity varies little with $p_\perp$ in the hemisphere centered around $p_\perp$ (toward) while it increases streadily in the away hemisphere. The phenomenon in the away hemisphere appears to be the same as already observed with large $p_\perp$ hadron triggers[9]. This is illustrated in Fig. 22, where the away hemisphere μ-pair data are compaired to data with a π^o trigger (both data are normalized at low $p_\perp$). Simply to indicate the type of arguments that can be made (and despite the rather low $p_\perp$ involved) we note that this would be understandable in a Compton scattering mechanism for μ-pair production and a quark-quark scattering mechanism for π^o production, since a quark jet would be recoiling against the trigger in both cases. The situation should be different in the toward hemisphere, since - contrary to the μ-pair - the π^o is only one part of the accompaining jet. The comparison in the toward hemisphere is shown in fig. 23, where one can indeed find an indication for different behaviours, consistent with the above observation. As a final comment, one should remark that these studies have been limited untill now to rather low transverse momenta, $p_\perp < 2.5$ GeV/c. The situation might well be different at larger $p_\perp$'s.

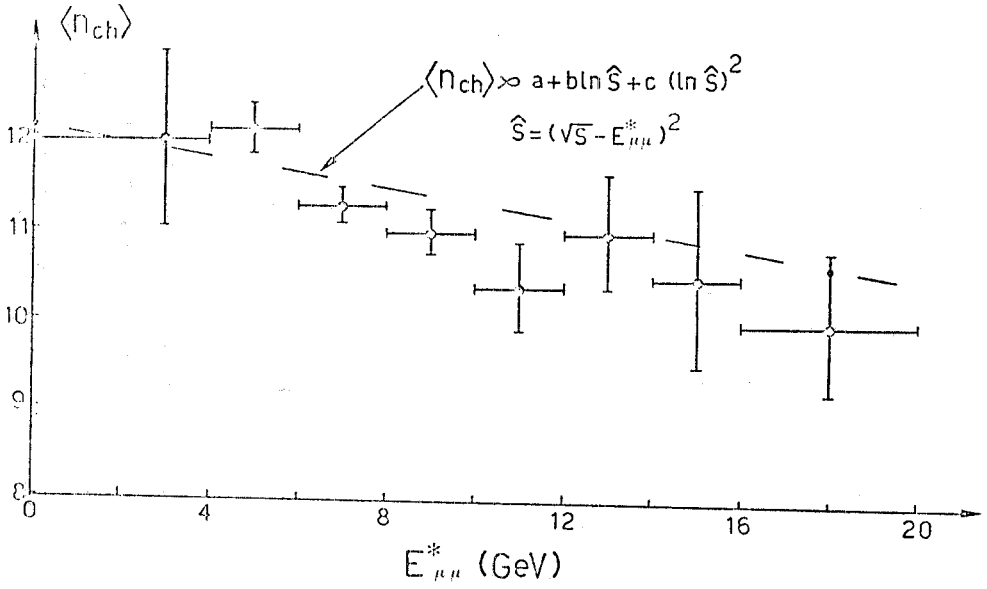

FIG. 20 - Raw mean charged multiplicity associated to heavy μ-pairs at $\sqrt{s}$ = 62 GeV as a function of the c.m.s. pair energy, from R209. The dotted curve shows the dependence of the inclusive multiplicity at the ISR[8], as a function of the reduced squared energy s (preliminary).

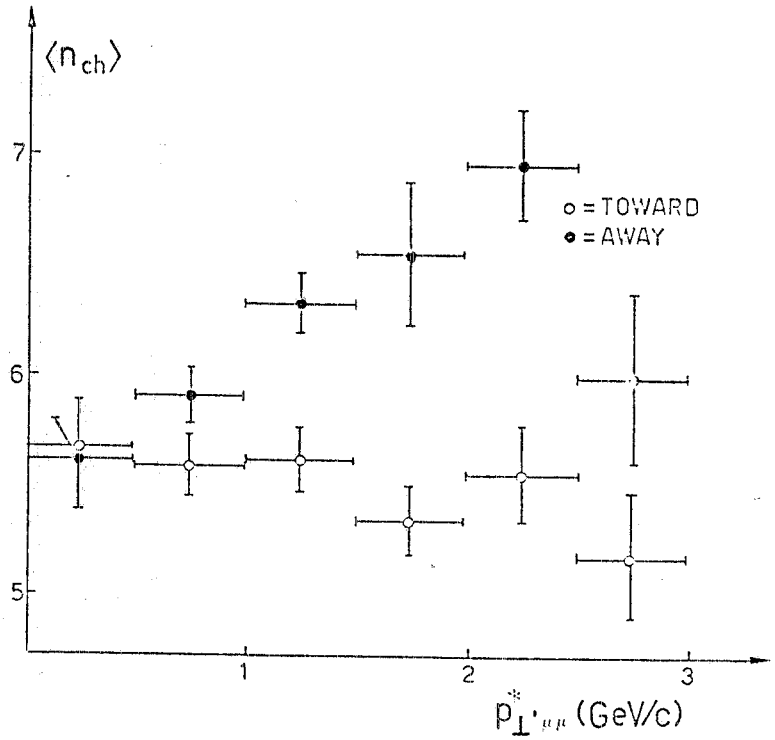

FIG. 21 - Raw mean charged multiplicity associated to heavy μ-pairs at $\sqrt{s}$ = 62 GeV as a function of the c.m.s. transverse momentum of the pair, in the toward ( ) and away ( ) hemispheres (from R209 , preliminary).

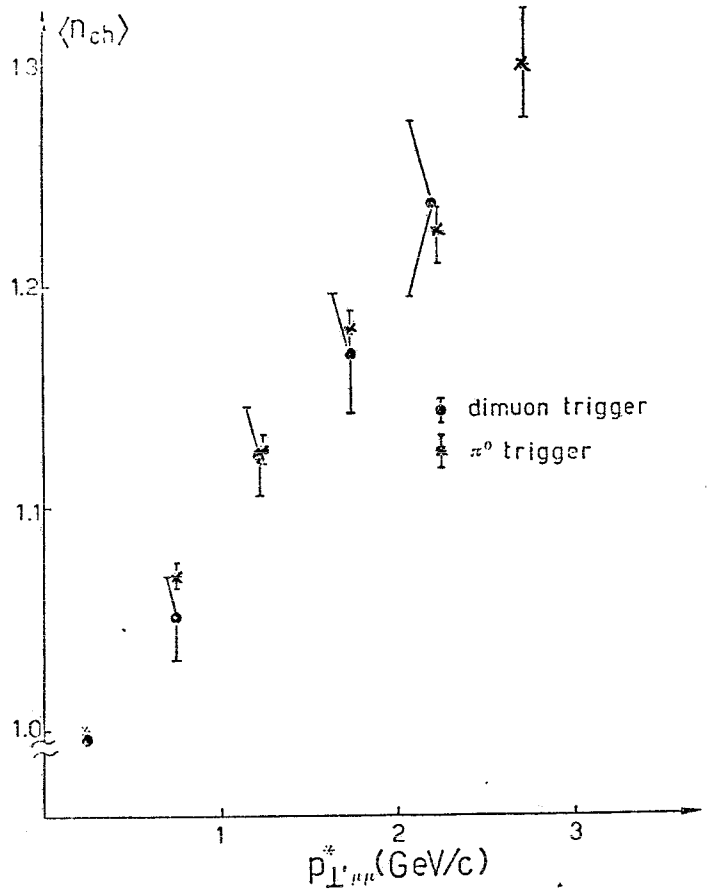

FIG. 22 - Dependence of the associated multiplicity in the c.m.s. hemisphere away from massive μ-pairs on the pair transverse momentum ($\sqrt{s}$ = 62 GeV data from R209, preliminary). ⧗ data from the Pisa-Stony Brook ISR experiment with a π^0 trigger, ref. 9. The data are normalized to the low $p_\perp \langle n_{ch} \rangle$.

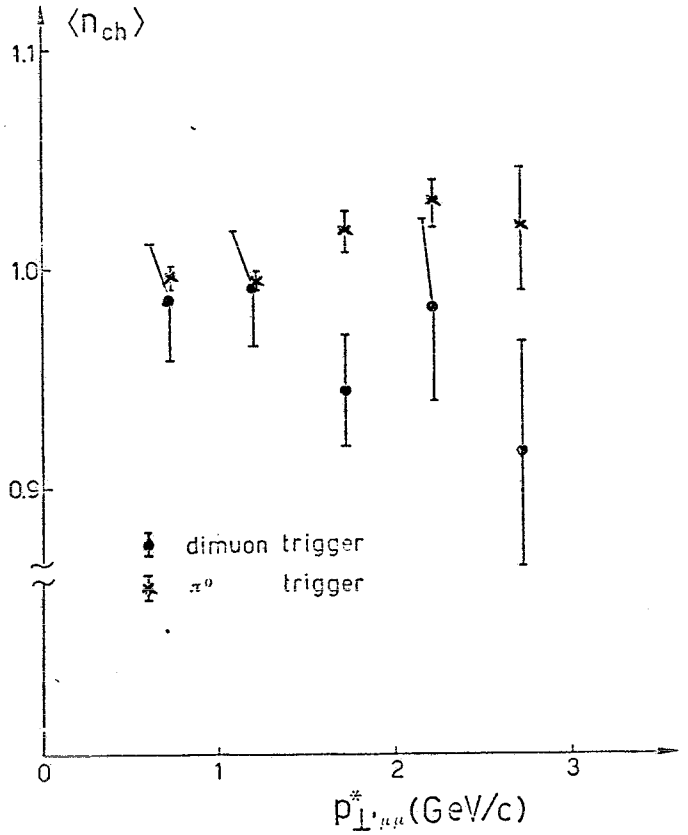

FIG. 23 - Dependence of the associated multiplicity in the c.m.s. hemisphere toward massive μ-pairs on the pair transverse momentum ($\sqrt{s}$ = 62 GeV data from R209, preliminary). ⧗ data with a π^0 trigger, ref. 9. The data are normalized to the low $p_\perp \langle n_{ch} \rangle$.

It is expected that experiments R108, R806, R209 will multiply their statistics by a factor of $2 \div 3$ at the end of data taking and analysis (end 1980). Informations of new type, rather than simply an increase of statistical accuracy, will possibly come from topical studies like large mass events, particle correlations, multi-lepton states, etc.

REFERENCES

(1) - S. D. Drell and T. M. Yan, Phys. Rev. Letters 25, 316 (1970).
(2) - L. M. Lederman, Proc. Intern. Conf. on High Energy Physics, Tokyo (1978), pag. 706.
(3) - F. Vannucci, Drell-Yan versus experiment, Proc. of the Karlsruhe Summer Institute, Karlsruhe (1978).
(4) - I. Mannelli, Lepton Pair Production Experiments at the ISR, Proc. of the 1979 Rencontre de Moriond (lepton week).
(5) - L. M. Lederman and B. G. Pope, Phys. Letters 66B, 486 (1977).
(6) - H. Newman, Proc. Intern. Conf. on High Energy Physics, Tokyo (1978) pag. 192.
(7) - F. Halzen, Proc. Intern. Conf. on High Energy Physics, Tokyo (1978) pag. 214.
(8) - W. Thomé, et al., Nuclear Phys. B129 (1977), 384
(9) - R. Kephart, et al., Phys. Rev. D14, 2909 (1976).